

# Constrained and Restrained Refinement in EXAFS Data Analysis with Curved Wave Theory

Norman Binsted, Richard W. Strange, and S. Samar Hasnain\*

*Molecular Biophysics Group, Daresbury Laboratory, Warrington, Cheshire WA4 4AD, U.K.*

*Received March 23, 1992; Revised Manuscript Received July 31, 1992*

**ABSTRACT:** This paper describes methods of constrained and restrained refinement of EXAFS data which provide a means of substantially reducing the number of independent parameters compared to conventional least-squares methods commonly used. Constrained refinement allows a major reduction in the number of free parameters for a refinement of a structural model. In restrained refinement, additional structural information from well-characterized small molecules is used to provide additional observations in the data analysis. Even though these methods are of general application to the majority of complex systems, they are particularly valuable for biological molecules. The methods are of major advantage for ligands where significant multiple scattering is present, e.g., histidine, tyrosine, CO, CN, etc. The bases of these methods are described, and applications to some complex chemical and biological systems are given.

X-ray absorption spectroscopy (EXAFS and XANES) has been widely used to provide information on the nature of metal centers in biological molecules (Cramer & Hodgson, 1979; Cramer, 1988; Scott, 1985; Hasnain, 1987, 1988; Hasnain & Garner, 1987; Blackburn, 1990; Lindley et al., 1990; Hedman et al., 1990). Analysis of biochemical systems using EXAFS often involves particular problems, due to both the experimental difficulties of using very low concentrations of the absorbing atom, which tends to limit the data range, and to the nature of the metal centers themselves. Metal sites in biological molecules are often coordinated by light elements, further reducing the useful data range both in *k*-space and *r*-space. The coordinating ligands also frequently include complex species such as histidine, for which the five atoms of the imidazole ring must be included in order to simulate the experimental spectrum (Bunker et al., 1982; Strange et al., 1986, 1987; Pettifer et al., 1986; Blackburn et al., 1987; Knowles et al., 1989). In histidine, as in other ligands containing ring complexes or near-colinear atomic positions, multiple scattering is very important, due to the focusing effect caused by the strong forward scattering from the nearest neighbor atom, and is responsible for enhancement of the EXAFS contribution from remote shells of atoms. Other ligands in which multiple scattering effects are important include pyridine, in which all the atoms are likely to contribute (Blackburn et al., 1988), and tyrosine, in which at least two of the phenolate carbons must be included as well as the nearest neighbor oxygen (Garratt, 1989; Hasnain & Strange, 1990).

In model compounds, where data quality is high, refinement of simple structures gives reasonable results. In biological molecules, the problem is compounded by relatively poor data, increased number of ligand types, and sometimes by higher static disorder. Typically, the large number of parameters required to describe all the contributing atoms cannot be justified by the information content of the EXAFS data alone, and thus quite often refinement is underdetermined. As a consequence, parameters in different shells become highly correlated, and a large number of similar solutions are possible, with no well-defined minimum. These may include solutions in which minor shells are essentially fitting noise or compensating for inadequacies in the theory and may give misleading results. In order to circumvent the problem of

parameter refinement in underdetermined systems, the following three approaches have been used.

1. Parameters may be restricted in some way, for example by assuming that all atoms of similar type at similar distances have the same Debye-Waller factor or that only integer values of occupation numbers are considered.
2. Shells of atoms, which, at the minimum, make statistically insignificant contributions to the spectrum, are excluded.
3. Groups of atoms comprising a well-defined unit such as an imidazole or phenolate ring can be refined as a rigid unit so only a single distance parameter, and perhaps one or more angular parameters, need be defined for the ligand.

The latter approach has been used with the plane wave approximation (Co & Hodgson, 1981) and full curved wave multiple scattering theory (Hasnain & Strange, 1990) and has been particularly successful for biological molecules. We have called this approach constrained refinement (Hasnain & Strange, 1990). It provides a means of including information derived from other structural techniques in the EXAFS analysis, allowing possible models to be tested and associated parameters to be refined. The technique of constrained refinement is also used in protein crystallography (Sussman et al., 1977), where underdeterminacy may also occur in low-resolution structure determinations.

Constrained refinement usually relies on well-established X-ray parameters or distances obtained from model compounds for distances within the unit. This has the disadvantage that small but significant variations in these distances between different compounds cannot be taken into account. Crystallographic distances are also rarely exactly the same as those obtained from EXAFS, largely due to the inexact treatment of disorder in EXAFS, leading to apparent shortening of bonds, and to difficulties in calculating potentials for molecular species. In order to resolve these difficulties with constrained refinement, we have introduced the method of restrained refinement to EXAFS data analysis. In this method, commonly practiced in protein crystallography (Hendrickson & Konnert, 1980), departure from a set of ideal interatomic distances is permitted, but differences between ideal and refined distances contribute to the mathematical function which is being minimized. Here we discuss the application of the methods of constrained and restrained refinement to the analysis of EXAFS data, with particular reference to their

use with biological molecules but realizing that these approaches are equally valid for any complex molecular system.

### LEAST-SQUARES REFINEMENT OF EXAFS DATA

Least-squares refinement during EXAFS curve-fitting involves minimization of the sum of squares of residuals given by

$$\Phi = \sum_i (1/\sigma_i^2)(\chi^{\text{exptl}}(k_i) - \chi^{\text{th}}(k_i))^2 \quad (1)$$

where  $\chi^{\text{exptl}}(k)$  and  $\chi^{\text{th}}(k)$  are the experimental and theoretical EXAFS. We normally take  $\sigma$  to be defined by

$$1/\sigma_i = k_i^n / \sum_j k_j^n |\chi_j^{\text{exptl}}(k_j)| \quad (2)$$

where  $n$  is selected so that  $k^n \chi^{\text{exptl}}(k)$  has an approximately constant amplitude over the data range used.

The amplitude term

$$\sum_j k_j^n |\chi_j^{\text{exptl}}(k_j)| \quad (3)$$

ensures that spectra of widely varying amplitudes produce values of  $\Phi$  of the same order of magnitude, simplifying the numerical methods employed.

We also have a facility, however, for reading in values of  $\sigma_i$  derived from experiment, for example by calculating the standard deviation during averaging of experimental spectra. This allows for better estimation of errors but requires careful selection of experimental count times to ensure that high  $k$  as well as low  $k$  data contribute significantly to the spectrum, thereby allowing accurate distance determinations. The use of an amplitude term also allows us to define an  $R$ -factor:

$$R = \sum_i (1/\sigma_i) (|\chi^{\text{exptl}}(k_i) - \chi^{\text{th}}(k_i)|) \times 100\% \quad (4)$$

which gives a meaningful indication of the quality of fit in  $k$ -space, even though a minimum in  $R$  does not necessarily mean a minimum in  $\Phi$ . Here,  $\sigma$  is always defined as in eq 2. There is clearly no absolute definition of a good fit. However, for complex chemical and biological molecules, we suggest that an  $R$ -factor of around 20% would normally be considered a good fit, to non-Fourier-filtered data, while an  $R$ -factor of greater than about 40% would be poor. Lower values of the  $R$ -factor can be achieved for model compounds.

An absolute index of goodness of fit, which takes account of the degree of overdeterminacy in the system, is given by the reduced  $\chi^2$  function (Bunker et al., 1991):

$$\epsilon_p^2 = [1/(N_i - p)](N_i/N) \sum_i (1/\sigma_i^2)(\chi^{\text{exptl}}(k_i) - \chi^{\text{th}}(k_i))^2 \quad (5)$$

where  $N_i$  is the number of independent data points and  $p$  is the number of parameters.  $N_i$  is normally less than the number of data points  $N$ , and in the case that the data from  $k_{\min}$  to  $k_{\max}$  are Fourier filtered using a window  $r_{\min}$  to  $r_{\max}$  it is given by

$$N_i = 2(r_{\max} - r_{\min})(k_{\max} - k_{\min})/\pi \quad (6)$$

$N_i/p$  provides a convenient means of quantifying the degree of determinacy of the system. Thus, a refinement with a value of less than unity for  $N_i/p$  cannot be justified as it would mean less than one observation per parameter. A value of more than unity indicates the overdeterminacy of the refine-

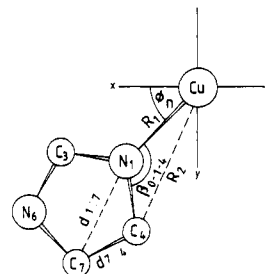


FIGURE 1: Imidazole ring showing the terminology used. Atomic positions are described either by spherical polar ( $r, \theta, \phi$ ) or Cartesian ( $x, y, z$ ) coordinates. The group is shown lying in the  $x$ - $y$  plane, with  $\theta = 90^\circ$  and  $z = 0^\circ$  for all atoms. The interatom distances, such as  $d_{7:4}$  between the  $C_7$  and  $C_4$  atoms, are the ideal distances obtained from many small molecule crystal structure determinations.

ment (Stout & Jenson, 1989). For typical enzyme data, 10–20 parameters can be justified on this basis.

### CONSTRAINED REFINEMENT

In constrained refinement, the number of parameters is reduced by treating a set of scattering atoms as a unit. A good example of a suitable unit is the five-atom imidazole group which shows only small variations in interatomic distances in more than 200 well-characterized chemical compounds (Orpen et al., 1989). By defining a unit, refinement of the position of the first nitrogen (bonded) atom and a single angular parameter,  $\beta$ , allows the position of the remaining atoms of the ligand to be simultaneously refined as the unit is essentially planar. Obviously, the coordination number of the whole ligand is defined by a single parameter. The number of Debye–Waller parameters can also be reduced by making the assumption that chemically similar atoms which are same distance away from the metal would have the same value. Thus, for a planar five-membered ring, three parameters define the Debye–Waller terms and one each defines the radial and angular position. The least-squares EXAFS refinement for a complex molecule containing imidazole groups should always be overdetermined in this case as  $N_i/p$  would be significantly increased.

### RESTRAINED REFINEMENT

In order to extend the refinement to include information derived from other techniques, we minimize:

$$\Phi = w_{\text{exafs}} \Phi_{\text{exafs}} + w_{\text{distances}} \Phi_{\text{distances}} + w_{\text{angles}} \Phi_{\text{angles}} \quad (7)$$

where  $w_{\text{exafs}}$ ,  $w_{\text{distances}}$ , and  $w_{\text{angles}}$  are the weighting factors used to define the relative significance of these contributions.  $\Phi_{\text{exafs}}$  is given as above;  $\Phi_{\text{distances}}$  and  $\Phi_{\text{angles}}$  are obtained by comparison of refined distances and angles with idealized distances and angles, which will often be obtained from an average of a large number of crystallographically characterized small molecules, as with the constrained refinement. At present, only certain angles,  $\beta$ , can be included as constraints. These are the angles where the vertex is the atom bonded to the central atom, and one apex is the central atom itself. For example, the parameters used to define an imidazole ring are shown in Figure 1.

The distance and angle contributions to the refinement are given by

$$\Phi_{\text{distances}} = \sum_i (1/\sigma_i^2)((r_i^{\text{ref}} - r_i^{\text{ideal}})/r_i^{\text{ideal}})^2 \quad (8)$$

with

$$1/\sigma_i = (1/\sigma_i^{\text{dist}}) / (\sum_j 1/\sigma_j^{\text{dist}}) \quad (9)$$

and

$$\Phi_{\text{angles}} = \sum_i (1/\sigma_i^2)(\beta_i^{\text{ref}} - \beta_i^{\text{ideal}})^2 \quad (10)$$

with

$$1/\sigma_i = (1/\sigma_i^{\text{ang}}) / (\sum_j 1/\sigma_j^{\text{ang}}) \quad (11)$$

Here  $r^{\text{ref}}$  refers to refined distances and  $r^{\text{ideal}}$  refers to idealized distances obtained from well-characterized small molecule structure determinations. The weightings  $w_{\text{exafs}}$ ,  $w_{\text{distances}}$ , etc. determine the relative significance of the EXAFS, distance, and angle contributions. The sum  $w_{\text{exafs}} + w_{\text{distances}} + w_{\text{angles}}$  must equal one. Although we have only implemented the restrained refinement for distance and angles, there are other possibilities. Examples are departure from planarity for ring complexes and comparison with crystallographic or theoretical Debye-Waller factors.

We also extend the definition of the  $R$ -factor to give

$$R = R_{\text{exafs}} + R_{\text{distances}} + R_{\text{angles}} \quad (12)$$

where  $R_{\text{exafs}}$  is defined as in eq 4 and the other terms are given by

$$R_{\text{distances}} = \sum_i (1/\sigma_i)(|r_i^{\text{ref}} - r_i^{\text{ideal}}|)/r_i^{\text{ideal}} \times 100 \quad (13)$$

and

$$R_{\text{angles}} = \sum_i (1/\sigma_i)(|\beta_i^{\text{ref}} - \beta_i^{\text{ideal}}|) \times 100 \quad (14)$$

In both  $\Phi$  and  $R$  the absolute values of  $\sigma$  do not affect the magnitude of the terms, only the relative values of  $\sigma$  within each category are significant. This is required as there is no obvious way of comparing experimental uncertainty with errors in bond lengths or angles. Defined in this way,  $R_{\text{distances}}$  corresponds to the percent mean error in bond length while  $R_{\text{angles}}$  is the absolute mean error in the angles in degrees. The values of  $\sigma$  for the restrained refinement can be derived from the standard deviation of crystallographic distances for small molecules, or by other means, including trial and error. Here we have assumed that bonded distances have  $1/\sigma$  equal to 5 and nonbonded distances have a  $1/\sigma$  of 2. These values allow the nonbonded distances to vary rather more than the bonded distances. Only interatomic distances within certain ligands are used. For other atom pairs,  $1/\sigma$  is set to zero so that they do not participate in the restrained refinement. We have not used the angle refinement in any of the examples presented here. The effect of the restrained refinement on the degree of determinacy is to increase the number of observations,  $N_i$ , although not of all the terms included will, in general, be independent. The number of independent observations generated by the addition of distance information is not necessarily the same as the number of bond lengths that are supplied because of correlations between them. The maximum number of additional independent observations is given by

$$\sum_i D(N_i - 2) + 1 \quad (15)$$

$D$  is the number of dimensions in which refinement takes place (1 for single scattering, 2 for planar groups, 3 for general refinement).  $N_i$  is the number of atoms per unit, and the sum  $i$  is over all units. It is assumed that the atom nearest to the center will have only one degree of freedom as EXAFS is invariant to translation of the unit in more than one dimension if only intraunit scattering paths are included. These observations will be weighted by  $1/\sigma$  as discussed above.

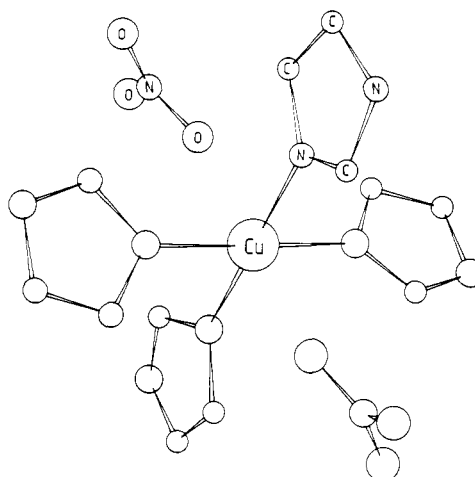


FIGURE 2: Structure of tetrakis(imidazolyl)copper(II) dinitrate.

Restrained refinement would be expected to give the same result as constrained refinement when  $w_{\text{distances}} = 1$ . The procedure used in performing the refinement will, however, be different, as the restrained refinement involves refining many more parameters. Both constrained and restrained refinement will therefore increase the determinacy: in one case by reducing  $p$  and in the other by tending to increase  $N_i$ .

#### REFINEMENT OF TETRAKIS(IMIDAZOLYL)-COPPER(II) DINITRATE

The sample preparation (McFadden et al., 1975) and acquisition of the K-edge spectrum at 77 K have been described previously (Strange et al., 1987), as has the calculation of theoretical phase shifts, which were also used for this work. Values for VPI (the constant imaginary part of the potential describing core-hole and final state lifetimes and experimental resolution) and AFAC (overall amplitude reduction due to many-electron and experimental effects) were also taken from previous work. The structure of this compound (McFadden et al., 1975) is shown in Figure 2. The copper site has  $C_1$  symmetry, with four approximately square planar imidazole nitrogens in the first shell and two oxygens from the axial nitrate groups at a slightly longer distance. In order to fit the EXAFS, the structure was idealized to give four equivalent planar imidazole groups and two equivalent nitrate groups. As no multiple scattering and therefore no angle dependence was included for intraligand paths, the attitude of the ligands is unimportant. For convenience it is assumed that the imidazole groups lie in the  $x$ - $y$  plane ( $\theta = 90^\circ$ ) and can be described by polar coordinates  $r$  and  $\phi$  and that the nitrate oxygen is at  $\theta = 0^\circ$  with the nitrogen at  $\theta \approx 30^\circ$ . Averaged crystallographic distances for the idealized structure are shown in Table I, column 1. All atoms are assumed to be coplanar with the central Cu atom. This results in small departures from the average bond angles in the idealized structure. The notation used to describe distances and angles within the imidazole ring is shown in Figure 1. Figure 3b shows the fit to theory obtained using the crystallographic values of distances and angles. The values of  $E_0$ , the difference between the edge position and the origin of the wave vector, and those of the Debye-Waller terms  $\alpha (=2\sigma^2)$  were refined. Seven shells were included (the imidazole groups plus the nitrate oxygen and nitrogen). Curved wave theory (Lee & Pendry, 1975; Gurman et al., 1984) was used including multiple scattering to third order for the 3-atom paths (Gurman et al., 1986; Binsted et al., 1987), in both the imidazole and nitrate groups, which included an angle of greater than  $120^\circ$ . The fit obtained

Table I: Best-Fit Parameters for  $\text{Cu}(\text{imid})_4(\text{NO}_3)_2^a$ 

parameters	X-ray				restrained			
	7 shells	5 shells	constrained	free	$w(\text{dist}) = 0.9$	$w(\text{dist}) = 0.75$	$w(\text{dist}) = 0.5$	$w(\text{dist}) = 0.25$
$E_0$	<b>15.6</b>	<b>15.6</b>	<b>17.0</b>	<b>17.3</b>	<b>17.2</b>	<b>17.3</b>	<b>17.3</b>	<b>17.2</b>
$R_1$	2.01	2.01	<b>2.00</b>	<b>2.00</b>	<b>2.00</b>	<b>2.00</b>	<b>2.00</b>	<b>2.00</b>
$R_2$	2.57		<b>2.37</b>	<b>2.40</b>	<b>2.37</b>	<b>2.38</b>	<b>2.38</b>	<b>2.39</b>
$R_3$	2.99	2.99	<b>2.94</b>	<b>2.92</b>	<b>2.94</b>	<b>2.93</b>	<b>2.92</b>	<b>2.92</b>
$R_4$	3.04	3.04	3.06	<b>3.02</b>	<b>3.06</b>	<b>3.05</b>	<b>3.03</b>	<b>3.02</b>
$R_5$	3.69							
$R_6$	4.14	4.14	4.11	<b>4.10</b>	<b>4.11</b>	<b>4.10</b>	<b>4.10</b>	<b>4.10</b>
$R_7$	4.19	4.19	4.19	<b>4.21</b>	<b>4.19</b>	<b>4.19</b>	<b>4.21</b>	<b>4.22</b>
$\alpha_1$	<b>0.004</b>	<b>0.004</b>	<b>0.003</b>	<b>0.004</b>	<b>0.003</b>	<b>0.003</b>	<b>0.003</b>	<b>0.003</b>
$\alpha_2$	<b>0.392</b>		<b>0.031</b>	<b>0.025</b>	<b>0.029</b>	<b>0.028</b>	<b>0.027</b>	<b>0.026</b>
$\alpha_{3/4}$	<b>0.008</b>	<b>0.010</b>	<b>0.001</b>	<b>0.007</b>	<b>0.002</b>	<b>0.003</b>	<b>0.003</b>	<b>0.005</b>
$\alpha_{6/7}$	<b>0.016</b>	<b>0.016</b>	<b>0.014</b>	<b>0.009</b>	<b>0.013</b>	<b>0.012</b>	<b>0.010</b>	<b>0.008</b>
$\phi_3$	339.3	339.3	<b>338.2</b>	<b>337.0</b>	<b>338.1</b>	<b>338.0</b>	<b>337.8</b>	<b>337.5</b>
$\phi_4$	21.1	21.1	20.2	<b>20.7</b>	<b>20.2</b>	<b>20.2</b>	<b>20.3</b>	<b>20.8</b>
$\phi_6$	350.1	350.2	348.8	<b>348.7</b>	<b>348.8</b>	<b>348.7</b>	<b>348.6</b>	<b>348.4</b>
$\phi_7$	9.3	9.3	7.9	<b>5.3</b>	<b>7.9</b>	<b>7.9</b>	<b>7.6</b>	<b>7.3</b>
$\beta_{0-1-3}$	126.5	126.5	123.8	121.1	123.7	123.4	122.6	122.1
$\beta_{0-1-4}$	-127.0	-127.0	-129.6	-127.7	-129.7	-129.4	-128.7	-127.7
$\beta_{0-1-6}$	161.2	161.2	158.6	158.3	158.5	158.4	158.1	157.8
$\beta_{0-1-7}$	-162.3	-162.2	-164.9	-170.0	165.0	-165.1	-165.6	-166.3
$R_{\text{exafs}}$	34.80	36.16	25.29	18.25	24.43	22.49	18.89	18.24
$R_{\text{distance}}$	0.00	0.00	0.00	3.92	0.04	0.29	0.96	1.53
$R_{\text{total}}$	34.80	36.16	25.29	22.17	24.47	22.78	19.85	19.77
$p$	6.0	4.0	8.00		15.0	15.0	15.0	15.0
$N_i$	21.5	21.5	21.5	21.5	28.5	28.5	28.5	28.5
$\Phi \times 10^3$	0.40	0.44	0.24	0.15	0.002	0.014	0.045	0.091
$\epsilon_p^2 \times 10^6$	1.31	1.25	0.90	1.18	0.02	0.11	0.35	0.70

<sup>a</sup>  $E_0$  is the edge position relative to the photoelectron wavevector;  $R_n$  and  $\alpha_n$  refer to the distances (in angstroms) and Debye–Waller terms (in  $\text{\AA}^2$ ) for shell  $n$ ;  $\Phi$ ,  $\epsilon$ ,  $N_i$ ,  $p$ ,  $R(\text{exafs})$ , and  $R(\text{distance})$  are defined in the main text.  $\phi_n$  is the polar angle for shell  $n$ . The corresponding  $\beta$  angles are also shown as they directly convey geometrical information. All refined parameters are shown in bold type.

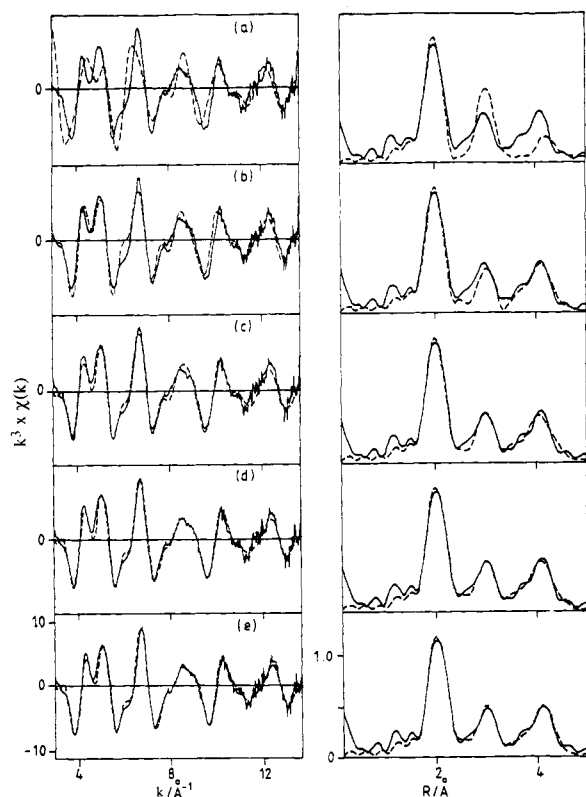


FIGURE 3: Best theoretical fit (left) and Fourier transform (right) with (a) single scattering and with multiple scattering using (b) crystal structure distances, (c) constrained refinement, (d) restrained refinement, and (e) free refinement. The solid line is the experimental; the dashed line is the theory.

using the distances from the room temperature crystal structure determination (McFadden et al., 1975) is characterized by  $R_{\text{exafs}} = 34.8\%$ . The parameters used are shown in Table I. Refined parameters are shown in bold type and  $\beta$  angles, as

defined in Figure 1, are given for convenience. The refined value of  $\alpha$  for both the nitrate atoms is very high, effectively removing the contribution of these atoms. Neither shell is statistically significant (Joyner et al., 1987), and essentially identical results were obtained by excluding them.

Refinement proceeded using the method of constrained refinement. The distance of the imidazole and the nitrate groups, the  $\phi$  coordinate of one of the imidazole carbons, and the Debye–Waller terms  $\alpha$  and  $E_0$  were included in the refinement. An additional constraint was that  $\alpha$  for the two pairs of proximal and distal atoms in the imidazole rings were forced to take the same value. This resulted in nine refinable parameters. The value of  $\alpha$  for the nitrate oxygen that was observed was  $0.031 \text{ \AA}^2$ . At this value, the shell is statistically significant at the 1% level, although the nitrogen shell was not significant at the 5% level. Subsequent refinements included the oxygen but not the nitrogen. In all refinements, the nitrate oxygen position refined to a much shorter distance than the room temperature crystallographic value and gave a far higher Debye–Waller term than the thermal parameters in X-ray structure would suggest. Inclusion of the oxygen also results in a lowering of  $\alpha$  for the proximal carbons of the imidazole—in some cases to unrealistically low values. Subsequent refinement of the remaining eight parameters resulted in an  $R_{\text{exafs}}$  of 25.3%. Table I shows the parameters used. The  $\beta$  angles were very close to the averaged crystallographic values, and the copper–imidazole distance was slightly shorter than the crystallographic value. With the exception of the proximal carbons, the Debye–Waller factors were all reasonable, considering the temperature of the experiment, the marked decrease in correlation of thermal motion with distance, and the static disorder contributing to the distal carbons and nitrogens.

Next, the refinement was repeated without any constraints. All the distances and angles were allowed to vary, together

Table II: Ideal and Refined Distances within the Imidazole Ring for Restrained and Free Refinement<sup>a</sup>

atom <i>I</i>	atom <i>J</i>	ideal	refined	error %
A. Restrained Refinement, $w(\text{dist}) = 0.5$				
3(C)	1(N)	1.316	1.310	0.49
4(C)	1(N)	1.372	1.351	1.52
4(C)	3(C)	2.154	2.162	-0.39
6(N)	1(N)	2.182	2.173	0.42
6(N)	3(C)	1.331	1.343	-0.88
6(N)	4(C)	2.185	2.203	-0.82
7(C)	1(N)	2.228	2.242	-0.64
7(C)	3(C)	2.192	2.215	-1.07
7(C)	4(C)	1.362	1.417	-3.99
7(C)	6(N)	1.382	1.377	0.31
B. Free Refinement				
3(C)	1(N)	1.316	1.321	-0.40
4(C)	1(N)	1.372	1.357	1.03
4(C)	3(C)	2.154	2.212	-2.69
6(N)	1(N)	2.182	2.173	0.44
6(N)	3(C)	1.331	1.375	-3.33
6(N)	4(C)	2.185	2.225	-1.82
7(C)	1(N)	2.228	2.238	-0.45
7(C)	3(C)	2.192	2.153	1.77
7(C)	4(C)	1.362	1.534	12.64
7(C)	6(N)	1.382	1.212	12.30

<sup>a</sup> Labeling of atoms is defined in Figure 1. Statistical errors are given in Table III.

with the Debye-Waller factors as before. The number of parameters in this case was 15. The quality of the fit as reflected by the *R*-factor improved substantially over the constrained refinement. The *R*-factor improved from 25.3% to 18.3%. However, a significant distortion of the ring takes place (Table II), and errors of as much as 12% occurred for distances between the ring atoms. The value of  $\epsilon_r^2$  is actually much larger than for the constrained refinement as the improvement in the fit is more than offset by the large increase in the number of parameters.

A restrained refinement was then performed with  $w_{\text{distances}} = 0.9, 0.75, 0.5$ , and  $0.25$ . These values resulted in refinements which varied from a near constrained refinement at  $w_{\text{distances}} = 0.9$  to a near unrestrained refinement at  $0.25$ . It can be seen that intermediate values of  $w_{\text{distances}}$  almost eliminate the distortion of the ring present in the unrestrained refinement, while achieving a significantly better fit to the data than is possible in the constrained refinement. A comparison of ideal and refined interatomic distances within the imidazole ring is given in Table II for  $w_{\text{distances}} = 0.5$ . The largest error for ring atoms distances in this case is 4% with an average error of  $\approx 1\%$ .

We have no objective criterion for selecting the optimum value of  $w_{\text{distances}}$ , and the value required may be dependent on the molecule being studied and on the quality of data. For proteins, however, it would appear that a reasonable approach would be to select the minimum value of  $w_{\text{distances}}$  for which the average departure from ideal distances is less than 1%, as this is similar to what is expected from the chemical variability and to errors in EXAFS distances. Here this criterion is achieved at  $w_{\text{distances}} = 0.5$ . At this value distortion of the ring is almost eliminated, but the quality of fit is scarcely reduced.

It is clear from this example that even though constrained refinement is well determined,  $N_i/p = 2.7$  (Stout & Jenson, 1989), the quality of fit to the EXAFS data is inferior to both the restrained and free refinements. Free refinement results in an unacceptable distortion of the imidazole ring while providing an excellent simulation of the EXAFS data. Restrained refinement is able to achieve simulation of the EXAFS data of similar quality but with a less than 1% deviation from ideal distances. The increase in observations

due to the inclusion of distance information results in a significant improvement in the overdeterminacy of the refinement;  $N_i/p$  increases from 1.4 for free refinement to 1.9 for the restrained refinement.

The correlation between two parameters is given by  $C_{ij}/(C_{ii}C_{jj})^{1/2}$  where  $C_{ij}$  etc. are elements of the standard covariance matrix  $C = [\Phi/(N-p)](A^t A)^{-1}$ , where  $\Phi$  is defined in eq 1,  $N$  is the total number of observations, and  $p$  is the number of parameters refined. Matrix  $A$  has elements  $A_{ij}$  given by  $\partial F_i / \partial x_j$ , where  $x_j$  etc. are the parameters and  $F_i$  are elements of the residual vector  $F_i = (1/\sigma_i^2)(\chi^{\text{exptl}}(k_i) - \chi^{\text{th}}(k_i))^2$ .

The correlation matrix and estimates of errors ( $2\sigma$ ) are shown in Table III for constrained, restrained ( $w_{\text{distances}} = 0.5$ ) and free refinements. In the case of free refinement, high correlations are observed for parameters defining atoms 4 and 6. The values of  $2\sigma$ , a measure of statistical uncertainty for a parameter, for the restrained refinement are in general substantially less than for the free refinement confirming a more satisfactory refinement. The "true" error of any parameter will, however, be larger than the  $2\sigma$  error due to the uncertainties in the EXAFS theory used (e.g., phase shifts), simplifying assumptions about structural symmetry, etc. A comparison between the averaged crystallographic distances and angles and the distances and angles obtained from refinement provides more information about the different methods of refinement employed here than do the  $2\sigma$  errors. The information summarized in Table II illustrates the most important point we wish to convey, namely, the superiority of restrained refinement over free refinement in achieving a satisfactory simulation of the EXAFS spectrum while retaining chemically sensible solutions.

## REFINEMENT OF CHLOROHEMIN

$\alpha$ -Chlorohemin is a synthetic iron-protoporphyrin-IX compound in which  $\text{Fe}^{3+}$ -porphyrin complexes are coordinated by Cl atoms at about 2.22 Å (Koeing, 1965). It was selected because the Fe lies out of the porphyrin plane, a phenomenon seen in hemoglobin (Fermi et al., 1984) and other proteins. The structure of the  $\alpha$ -chlorohemin is shown in Figure 4. The porphyrin complex is almost, but not quite, planar. As it is clearly impossible to refine the coordinates for the large number of atoms making significant contributions to the EXAFS, it is important to find a method by which the degree of out of plane displacement can be evaluated using EXAFS.

Chlorohemin was prepared by published methods (Koeing, 1965). The Fe K-edge spectrum was measured in fluorescence mode (Figure 5). Phase shifts, and the constant imaginary potential VPI, were as for earlier work on hemoglobin (Perutz et al., 1982). In order to fit the experimental spectrum, the structure was idealized to give  $C_4$  symmetry at the central atom. The chlorine, the atoms of the pyrrole rings, and the bridging carbons were included, together with a single shell of carbons from an adjacent porphyrin complex. The porphyrin side chains were not significant and were excluded. Multiple scattering paths to third order involving angles of greater than  $120^\circ$  were included for a unit defined as one-fourth of the porphyrin group. The spectrum was fitted initially using constrained refinement (Table IV). This involved refining the  $x$  and  $z$  coordinate of the nitrogen, together with the polar  $\phi$  coordinate of one of the pyrrole carbons and the radial distance of the chlorine and the additional carbons. These parameters were selected so that out-of-plane movement could be refined. This permitted the Fe-porphyrin distance, the displacement of the Fe from the

Table III: Correlations between Variables for Different Methods of Refinement<sup>a</sup>

A. Constrained Refinement								
	$E_0$	$R_1$	$R_2$	$\alpha_1$	$\alpha_2$	$\alpha_{3/4}$	$\alpha_{6/7}$	$\phi_3$
$R_1$	-0.45	1						
$R_2$	0.08	0.08	1					
$\alpha_1$	0.06	-0.05	0.21	1				
$\alpha_2$	-0.18	0.18	-0.12	0	1			
$\alpha_{3/4}$	0.25	-0.14	0.19	-0.02	-0.20	1		
$\alpha_{6/7}$	-0.28	0.15	-0.21	-0.09	0.08	-0.4	1	
$\phi_3$	-0.26	0.18	-0.30	-0.06	0.08	-0.61	0.59	1
$2\sigma$	0.29	0.002	0.018	0.000	0.006	0.002	0.002	0.828

B. Restrained Refinement, $w(\text{dist}) = 0.5$															
	$E_0$	$R_1$	$R_2$	$R_3$	$R_4$	$R_6$	$R_7$	$\alpha_1$	$\alpha_2$	$\alpha_{3/4}$	$\alpha_{6/7}$	$\phi_3$	$\phi_4$	$\phi_6$	$\phi_7$
$R_1$	-0.68	1													
$R_2$	0.08	-0.01	1												
$R_3$	-0.43	0.28	-0.18	1											
$R_4$	-0.33	0.26	-0.14	-0.05	1										
$R_6$	-0.60	0.40	-0.04	0.39	0.04	1									
$R_7$	-0.40	0.28	-0.06	0.20	0.15	-0.25	1								
$\alpha_1$	0.03	-0.06	0.20	0.11	-0.21	0.07	-0.02	1							
$\alpha_2$	-0.32	0.04	-0.09	0.16	0.17	0.20	0.14	-0.20	1						
$\alpha_{3/4}$	0.08	-0.08	-0.01	0.50	-0.76	0.15	-0.03	0.17	-0.14	1					
$\alpha_{6/7}$	-0.24	0.15	-0.03	0.07	0.11	0.68	-0.59	-0.01	-0.09	-0.07	1				
$\phi_3$	-0.27	0.17	-0.09	0.37	-0.24	0.27	0.23	0.06	0.16	0.26	0.03	1			
$\phi_4$	0.15	-0.10	0.09	0.13	-0.60	0.06	-0.05	0.08	-0.02	0.50	-0.13	0.49	1		
$\phi_6$	-0.07	0.04	0.02	0.29	-0.47	0.29	-0.06	0.10	0.06	0.45	0.02	0.64	0.74	1	
$\phi_7$	-0.01	-0.01	0.02	0.26	-0.48	0.27	-0.15	0.10	0.04	0.44	0.05	0.62	0.72	0.93	1
$2\sigma$	0.456	0.002	0.014	0.006	0.010	0.014	0.014	0.000	0.006	0.002	0.004	0.376	0.420	0.484	0.474

C. Free															
	$E_0$	$R_1$	$R_2$	$R_3$	$R_4$	$R_6$	$R_7$	$\alpha_1$	$\alpha_2$	$\alpha_{3/4}$	$\alpha_{6/7}$	$\alpha_3$	$\alpha_4$	$\alpha_6$	$\alpha_7$
$R_1$	-0.77	1													
$R_2$	0.06	-0.03	1												
$R_3$	-0.08	0.06	0.02	1											
$R_4$	-0.21	0.15	-0.20	-0.80	1										
$R_6$	-0.66	0.51	-0.01	-0.01	0.15	1									
$R_7$	-0.16	0.14	0.04	-0.07	-0.01	0.21	1								
$\alpha_1$	0.04	-0.06	0.18	0.16	-0.15	0.00	-0.03	1							
$\alpha_2$	-0.40	0.18	-0.06	0.00	0.12	0.35	0.26	-0.04	1						
$\alpha_{3/4}$	0.17	-0.13	0.13	0.89	-0.95	-0.17	-0.10	0.13	-0.15	1					
$\alpha_{6/7}$	-0.51	0.39	-0.13	-0.05	0.27	0.44	-0.58	-0.03	0.10	-0.21	1				
$\phi_3$	-0.42	0.36	0.01	-0.08	0.03	0.51	0.59	-0.10	0.41	-0.17	-0.01	1			
$\phi_4$	-0.16	0.14	0.22	0.25	-0.46	0.27	0.43	-0.06	0.26	0.34	-0.23	0.73	1		
$\phi_6$	0.04	-0.03	0.04	-0.22	0.11	0.40	0.78	-0.02	0.18	-0.21	-0.53	0.46	0.29	1	
$\phi_7$	0.26	-0.19	0.15	0.25	-0.43	-0.49	0.15	-0.01	-0.02	0.39	-0.61	0.14	0.48	-0.01	1
$2\sigma$	0.518	0.002	0.012	0.014	0.024	0.028	0.020	0.000	0.004	0.006	0.006	1.52	1.62	7.36	2.58

<sup>a</sup>  $E_0$  is the edge position relative to the origin of the photoelectron wavevector;  $R_n$ ,  $\alpha_n$ , and  $\phi_n$  refer to distances, Debye-Waller terms, and polar angles, respectively, for shell  $n$ . Shell sequences are the same as for Table I.  $2\sigma$  is twice the square root of the variance, a measure of the statistical uncertainty of the refined values.

porphyrin plane, and the rotation of the pyrrole ring to be optimized. The planarity of the porphyrin was forced to be maintained, but the longer of the two bridging distances

between pyrrole groups could vary. Together with the Debye-Waller terms, this gave 12 refinable parameters. The parameters shown in Table IV are the radial distances and  $\beta$

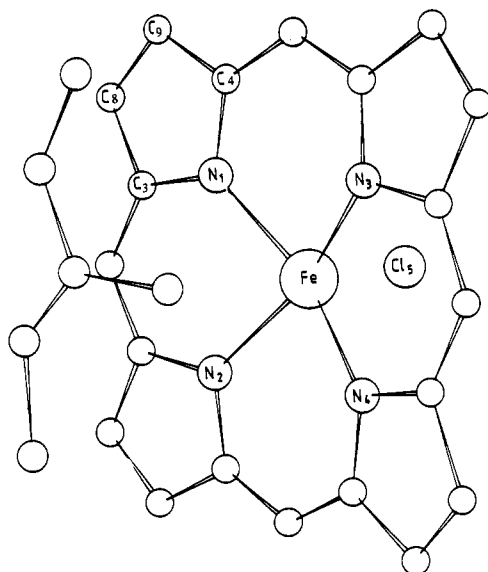


FIGURE 4: Structure of chlorohemin.

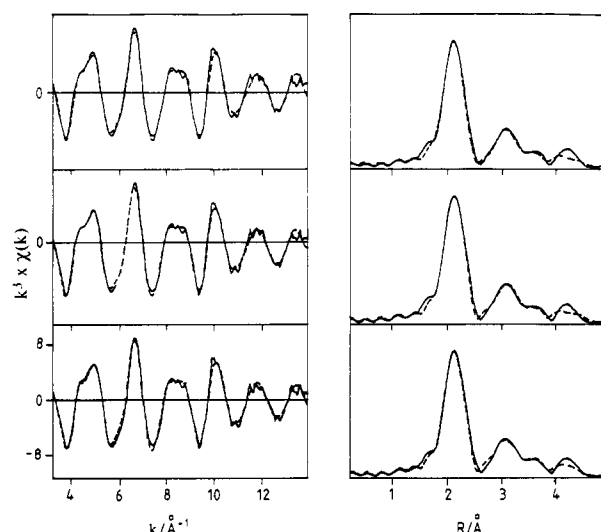


FIGURE 5: Best theoretical EXAFS fit (left) and Fourier transform (right) for chlorohemin for (a) multiple scattering, using distances from the crystal structure, (b) constrained refinement, and (c) restrained refinement with  $w_{\text{dist}} = 0.8$ . The solid line is the experimental; the dashed line is the theory.

angles resulting from this refinement, which gave a surprisingly good fit, with an  $R$ -factor of 13.6%. The out of plane distance of 0.59 Å was somewhat larger than the mean crystallographic distance of 0.48 Å, but the agreement is considered good as EXAFS is rather insensitive to such distances. In order to check the uniqueness of the out of plane distance, we performed the refinement with  $z$  initially zero and then with  $z$  a large value. Both models gave the  $z$  value within 0.01 Å.

A free refinement was then performed, starting from the result of the constrained refinement. The atomic positions were allowed to move in three dimensions, except for the nearest atoms in the porphyrin group and the isolated chlorine and carbons in which only the radial distances were refined. These atoms were restricted to one dimension, as EXAFS is completely insensitive to translational motion of units in more than one dimension if interligand multiple scattering paths are excluded. As expected, although allowing a good fit to the data, the results of this refinement were unacceptable: the negative value of  $\epsilon_v^2$  (Table IV) shows that the refinement was highly underdetermined, and the distortion of the ring (Figure 6), causing it to become markedly nonplanar, is chemically impossible. The statistical errors are also extremely

Table IV: Best-Fit Values for Chlorohemin for Simulations Based on the Averaged Crystallographic Structure, Constrained, Free, and Restrained Refinements<sup>a</sup>

parameters	X-ray	constrained	free	restrained
$E_0$	17.6	20.9	20.0	20.3
$R_1$	2.06	2.04	2.05	2.05
$R_2$	2.22	2.19	2.19	2.19
$R_3$	3.09	3.06	3.01	3.02
$R_4$	3.10	3.06	3.12	3.13
$R_5$	3.46	3.43	3.42	3.42
$R_{6/7}$	3.85	3.77	3.82	3.83
$R_8$	4.31	4.27	4.13	4.16
$R_9$	4.31	4.27	4.33	4.29
$\alpha_1$	0.004	0.009	0.008	0.009
$\alpha_2$	0.004	0.001	0.002	0.002
$\alpha_{3/4}$	0.008	0.009	0.001	0.001
$\alpha_5$	0.015	0.007	0.004	0.008
$\alpha_{6/7}$	0.013	0.007	0.010	0.009
$\alpha_{8/9}$	0.041	0.028	0.017	0.009
$\beta_{0-1-3}$	-126.2	-125.6	-128.1	-121.9
$\beta_{0-1-4}$	126.3	125.5	122.4	128.9
$\beta_{0-1-5}$	99.6	99.2	98.0	99.6
$\beta_{0-1-8}$	158.7	156.6	144.2	149.4
$\beta_{0-1-9}$	-158.7	-156.8	-166.8	-155.3
$z_1$	0.48	0.59	0.60	0.60
$R_{\text{exafs}}$	21.8	13.6	11.5	13.2
$R_{\text{distance}}$	0	0	5.69	0.96
$R_{\text{total}}$	21.8	13.6	17.2	14.1
$p$	7	12	25	25
$N_i$	21.6	21.6	21.6	32.6
$\Phi \times 10^3$	0.428	0.197	0.133	0.017
$\epsilon_v^2 \times 10^6$	3.91	2.73	-4.8	0.41

<sup>a</sup>  $z_1$  is the displacement in angstroms of the Fe atom from the porphyrin plane. Other parameters are as defined in Table I.

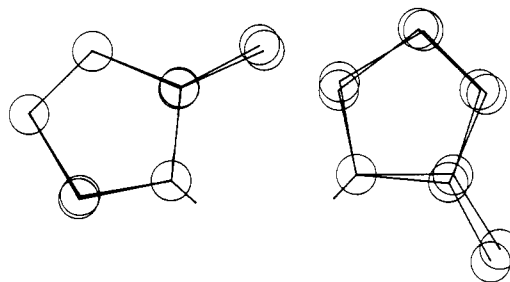


FIGURE 6: Distortion of the pyrrole rings for the restrained (left) and free (right) refinement.

large. The distortion is largely due to out of plane movement of the middle pair of carbon atoms and result in an average departure of 5.7% from the ideal distances.

A restrained refinement, starting from the unrestrained coordinates, with  $w_{\text{distance}} = 0.8$  was then performed. The weights were chosen so as to give  $R_{\text{distance}}$  of  $\approx 1\%$ . The restrained refinement reduced the degree of distortion of the ring to a more reasonable level while allowing a good fit to the data. The  $R$ -factor for the restrained refinement is 13.2%. A lower value of  $w_{\text{distance}}$  gives a lower  $R$ -factor to the EXAFS data but results in an increased  $R_{\text{distance}}$  and subsequently in an increased distortion of the porphyrin. Values of  $N_i/p$  and  $\epsilon_v^2$  show that the situation is much improved for the restrained refinement compared to the free refinement. However, the overdeterminacy is not as good as  $\text{Cu}(\text{imid})_4(\text{NO}_3)_2$  where  $N_i/p$  was 1.9 compared to 1.25 in the present case. This reduction is due to the increased number of parameters required to allow displacement of each of the atoms from the porphyrin plane. The ring distortion is still significant and unrelated to the known structure. A restrained refinement in which only the  $z$  parameter for all of the atoms was refined gave essentially the same result as the constrained refinement and therefore had no advantage over the simpler and faster

Table V: Parameters Used in the Constrained and Restrained Refinement of Human Fetal Deoxyhemoglobin

parameters	constrained	restrained ( $w(\text{dist}) = 0.38$ )
$E_0$	23.9	23.8
$Z_1$	0.57	0.57
$X_1$	1.98	1.98
$R_1$	2.06	2.06
$R_2$	3.08	3.04
$R_3$	3.09	3.09
$R_4$	3.46	3.44
$R_5$	4.30	4.30
$R_6$	4.30	4.29
$R_7$	1.91	1.92
$R_8$	2.86	2.80
$R_9$	2.98	3.02
$R_{10}$	4.02	4.01
$R_{11}$	4.11	4.13
$\alpha_1$	0.006	0.006
$\alpha_{2/3}$	0.007	0.006
$\alpha_4$	0.015	0.016
$\alpha_{5/6}$	0.007	0.007
$\alpha_7$	0.002	0.002
$\alpha_{8/9}$	0.005	0.004
$\alpha_{10/11}$	0.013	0.010
$\beta_{0-1-2}$	-125.8	-124.5
$\beta_{0-1-3}$	125.9	127.5
$\beta_{0-1-4}$	99.6	100.1
$\beta_{0-1-5}$	156.9	156.0
$\beta_{0-1-6}$	-156.9	-157.5
$\beta_{0-7-8}$	-123.7	-121.1
$\beta_{0-7-9}$	129.9	132.7
$\beta_{0-7-10}$	-158.4	-155.4
$\beta_{0-7-11}$	165.2	168.0
$R_{\text{exafs}}$	30.3	27.8
$R_{\text{distance}}$	0	1.01
$R_{\text{total}}$	30.3	28.8
$N_i$	14.7	30.7
$p$	13	28
$\Phi \times 10^3$	0.507	0.176
$\epsilon_p^2 \times 10^6$	13.68	5.79

constrained method. Thus, it is clear that a three-dimensional refinement should be avoided for planar groups and that although both constrained and restrained refinements are able to determine the out of plane movement of the central atom, neither method is able to define the subtle distortion of the planar rings sometimes encountered in biological molecules.

## FETAL HEMOGLOBIN

X-ray crystallography has shown that in the liganded ( $\text{O}_2$  or CO) hemoglobins the  $\text{Fe}^{2+}$  atom lies in the mean porphyrin plane but that in (adult) deoxyhemoglobin the iron atom lies approximately 0.5 Å out of the plane (Fermi et al., 1984). In this section, we apply the methods described above to the EXAFS of fetal deoxyhemoglobin. We assume initially that the Fe atom will lie out of the mean porphyrin plane, as is the case for adult deoxyhemoglobin, and therefore the model compound described in the previous section will be a suitable starting point for defining the geometry of the pyrrole rings. The Cl atom of  $\alpha$ -chlorohemin is replaced by imidazole. There are therefore two multiple scattering units: the pyrrole, which represents one-fourth of the porphyrin unit, and the imidazole, which represents the proximal histidine of the averaged hemoglobin binding site. We used the same phase shifts, constant imaginary potential, and amplitude reduction factor as for  $\alpha$ -chlorohemin. Initial fitting was carried out using constrained refinement. This involved refining 13 parameters:  $E_0$ , the imidazole first shell distance and Debye–Waller term, the polar angle  $\phi$  of one of the second shell imidazole atoms, the Debye–Waller terms of the second and third shell

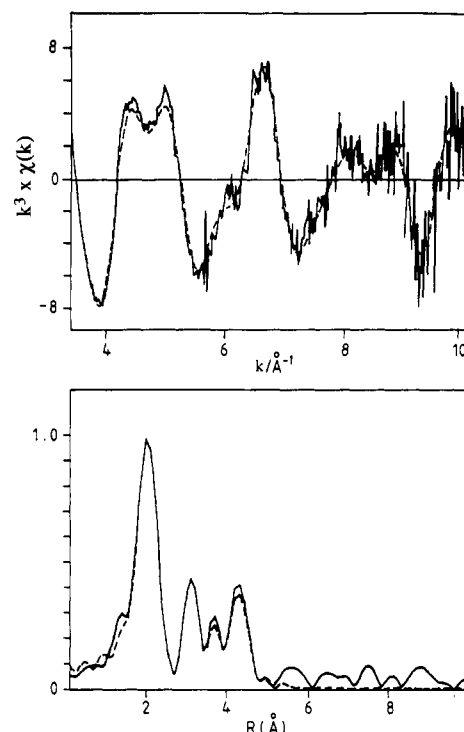


FIGURE 7: Restrained refinement of fetal deoxyhemoglobin. The solid line is the experimental; the dashed line is the theory.

atoms, the  $x$  and  $z$  values of the first shell porphyrin atom, the  $\phi$  parameter of one of the pyrrole carbon atoms, and the four Debye–Waller parameters of the pyrrole unit. The large number of parameters (13) for constrained refinement is just within the allowed number of independent parameters for this case (14.7), calculated using eq 6. The result of the constrained refinement gave an Fe– $N_{\text{porphyrin}}$  distance of 2.06 Å with the Fe atom 0.57 Å out of the porphyrin plane. The Fe– $N_{\text{imidazole}}$  distance refined to 1.91 Å. The  $R$ -factor was 30% and  $\epsilon_p^2 = 13.6$ . The fitting parameters are all shown in Table V. The simulation was also repeated from a different starting position, namely, with the Fe atom in the porphyrin plane, and the same result was obtained.

A restrained refinement of the data (Figure 7) was also carried out starting from the result of the constrained refinement. In this case, the total number of parameters being refined was 28: viz., all the above parameters plus the remaining radial distances, the  $\phi$  angles of the imidazole ring, and the  $\phi$  angles of the pyrrole ring. The  $\theta$  angles of the imidazole and porphyrin were not refined as these units were assumed to be planar—the simulations for chlorohemin above demonstrated that there was no advantage in allowing three-dimensional movement. The maximum number of allowed parameters in this case was calculated from eq 15. For the pyrrole unit, the maximum number of additional independent points is 9; for imidazole, the maximum number of additional independent points is 7. Thus, the total number of independent points is 30.7. Therefore, although the number of parameters being refined has more than doubled compared with constrained refinement, the problem is still just overdetermined. The refinement was carried out using  $w_{\text{distances}} = 0.38$ . The  $R$ -factor reduced to 27.8% and  $\epsilon_p^2$  decreased by about 230% to 5.8. There is clearly a significant element of noise in the raw data contributing to the value obtained for the  $R$ -factor. Values of  $N_i/p$  for both the constrained and restrained refinements are  $\approx 1.1$ ; thus, a free refinement would have been meaningless in this case.



## DISCUSSION

The results clearly show that constrained and restrained refinements are effective in permitting a good fit to the data while eliminating chemically impossible solutions. Indeed, the restrained refinement fits in which the mean departure from ideal distances is less than 1% are almost as good as those for the free refinement, which give rise to significant departure from reasonable distances. The addition of the extra observations also prevents overparameterization of the problem and results in a better defined minimum and faster convergence of the refinement. In cases where data quality and range is limited, constrained refinement has a major advantage. For complex systems, where data range is reasonable, use of restrained refinement should allow determination of real stereochemical differences.

It might be expected that additional observations would necessarily reduce the correlations between variables during refinement. This need not be the case, however, as correlations can also arise through an inappropriate choice of parameters. In the ideal case that the residual function  $F_i$  is approximately linear in all parameters  $x_i$  close to the minimum, then an equal valued surface of  $\Phi$  is ellipsoidal in  $n$ -dimensional space, and the optimal set of parameters corresponds to the orthogonal principal axes of the ellipsoid. These will not in general be the theory parameters which are usually selected. They may, for example, be linear combinations of two or more parameters. Although for single scattering the radial distances  $r$  are normally a good choice, for multiple scattering and for restrained refinement the interatomic vectors  $|r_n - r_m|$  are more important. Although multivariate techniques exist for selecting the best set of parameters, these have not been used. The parameters required will differ for each system studied and apply only closely to a minimum and would make data analysis more complex.

The importance of multiple scattering itself in ensuring chemically reasonable distances should not be underestimated. Multiple scattering, especially the higher orders, increases rapidly as the argument of the Hankel functions  $h(kr)$  decreases. This ensures that unrealistically short distances are automatically avoided. In general we restrict both the order and number of paths included for computational efficiency. Those paths which are not included are either insignificant in the EXAFS region or tend to cancel each other out (Gurman et al., 1986). For structures in which distances are too short, however, other contributions may be very large, and provided that sufficient paths are included in the refinement stereochemically improbable results will be avoided, at the expense of a considerable increase in computational effort.

## CONCLUSIONS

Constrained and restrained refinements offer the possibility of reliable structure determination from the EXAFS data of complex chemical and biochemical systems. The overdetermination of a refinement is increased either by reducing the number of free parameters or by increasing the number of observations by including chemical information from small molecule crystal structure data. Similar approaches have played a major role in the ability to refine crystal structure data for proteins over the last 15 years, and much has been learned from these structures. In principle, these approaches should enable one to extract more structural information than has been possible to date from a typical analysis of EXAFS data.

## REFERENCES

- Binsted, N., Cook, S. L., Evans, J., Greaves, G. N., & Price, R. J. (1987) *J. Am. Chem. Soc.* 109, 3669.
- Blackburn, N. J., Strange, R. W., McFadden, L. M., & Hasnain, S. S. (1987) *J. Am. Chem. Soc.* 109, 7162.
- Blackburn, N. J., Strange, R. W., Farooq, A., Haka, M. S., & Karlin, K. D. (1988) *J. Am. Chem. Soc.* 110, 4263.
- Blackburn, N. J. (1990) *Synchrotron Radiation and Biophysics* (Hasnain, S. S., Ed.) p 63, Ellis Horwood Ltd., Chichester, U.K.
- Bunker, G., Stern, E. A., Blakenship, R. E., & Parson, W. W. (1982) *Biophys. J.* 37, 539.
- Bunker, G., Bunker, B. A., Crozier, D., Goulon, J., Gurman, S. J., Hasnain, S. S., Heald, S. M., Koningsberger, D. C., Natoli, R., Rehr, J. R., Sayers, D., & Udagawa, Y. (1991) *X-Ray Absorption Fine Structure* (Hasnain, S. S., Ed.) p 751, Ellis Horwood Ltd., Chichester, U.K.
- Co, M. S., & Hodgson, K. O. (1981) *J. Am. Chem. Soc.* 103, 3200.
- Cramer, S. P. (1988) *X-Ray Absorption* (Koningsberger, D. C., & Prins, R., Eds.) p 257, John Wiley & Sons, New York.
- Cramer, S., & Hodgson, K. O. (1979) *Prog. Inorg. Chem.* 25, 1.
- Fermi, G., Perutz, M. F., Shaanan, B., & Fourme, R. (1984) *J. Mol. Biol.* 175, 159.
- Garratt, R. C. (1989) Ph.D. Thesis, Birkbeck College, University of London.
- Gurman, S. J., Binsted, N., & Ross, I. (1984) *J. Phys. C* C17, 143.
- Gurman, S. J., Binsted, N., & Ross, I. (1986) *J. Phys. C* C19, 1845.
- Hasnain, S. S. (1987) *Life Chem. Rep.* 4, 273.
- Hasnain, S. S. (1988) *Top. Curr. Chem.* 147, 73.
- Hasnain, S. S., & Garner, C. D. (1987) *Prog. Biophys. Mol. Biol.* 50, 47.
- Hasnain, S. S., & Strange, R. W. (1990) *Biophysics and Synchrotron Radiation* (Hasnain, S. S., Ed.) p 104, Ellis Horwood Ltd., Chichester, U.K.
- Hedman, B., Hodgson, K. O., & Garner, C. D. (1990) *Synchrotron Radiation and Biophysics* (Hasnain, S. S., Ed.) p 43, Ellis Horwood Ltd., Chichester, U.K.
- Hendrickson, W. A., & Konnert, J. H. (1980) *Biophys. J.* 32, 645.
- Joyner, R. W., Martin, K. J., & Meehan, P. (1987) *J. Phys. C* 20, 4005.
- Knowles, P. F., Strange, R. W., Blackburn, N. J., & Hasnain, S. S. (1989) *J. Am. Chem. Soc.* 111, 102.
- Koeing, D. F. (1965) *Acta Crystallogr.* 18, 633.
- Lee, P. A., & Pendry, J. B. (1975) *Phys. Rev. B* 11, 2795.
- Lindley, P. F., Garratt, R. C., & Hasnain, S. S. (1990) *Synchrotron Radiation and Biophysics* (Hasnain, S. S., Ed.) p 63, Ellis Horwood Ltd., Chichester, U.K.
- McFadden, D. L., McPhail, A. T., Garner, C. D., & Mabbs, F. F. (1975) *J. Chem. Soc., Dalton Trans.*, 263.
- Orpen, A. G., Brammer, L., Allen, F. H., Kennard, O., Watson, D. G., & Taylor, R. (1989) *J. Chem. Soc., Dalton Trans. Suppl.*, S1.
- Perutz, M. F., Hasnain, S. S., Duke, P. J., Sessler, J. L., & Hahn, J. E. (1982) *Nature* 295, 535.
- Pettifer, R. F., Foulis, D. L., & Hermes, C. (1986) *J. Phys. C* 8, 545.
- Scott, R. A. (1985) *Methods Enzymol.* 117, 414.
- Stout, G. H., & Jensen, L. H. (1989) *X-Ray Structure Determination*, New York, John Wiley & Sons.
- Strange, R. W., Blackburn, N. J., Knowles, P. F., & Hasnain, S. S. (1987) *J. Am. Chem. Soc.* 109, 7157.
- Strange, R. W., Hasnain, S. S., Blackburn, N. J., & Knowles, P. F. (1986) *J. Phys. C* 8, 593.
- Sussman, J. L., Holbrook, S. R., Church, G. M., & Kim, S.-H. (1977) *Acta Crystallogr. A* (33), 800.